Proceedings of the ASME 2019 Heat Transfer Summer Conference
HT2019
July 14-17, 2019, Bellevue, WA, USA

HT2019-3703

ON THE STEFAN PROBLEM WITH INTERNAL HEAT GENERATION AND PRESCRIBED HEAT FLUX CONDITIONS AT THE BOUNDARY

Lyudmyla Barannyk
Department of Mathematics
University of Idaho
Moscow, Idaho, 83843, USA
Email: barannyk@uidaho.edu

Sidney D. V. Williams
Moscow High School
Moscow, Idaho, 83843, USA
Email: sidneywilliams1231@gmail.com

Olufolahan Irene Ogidan
Department of Mathematics
University of Idaho
Moscow, Idaho, 83843, USA
Email: ogid1420@vandals.uidaho.edu

John C. Crepeau
Department of Mechanical Engineering
University of Idaho
Moscow, Idaho, 83843, USA
Email: crepeau@uidaho.edu

Alexey Sakhnov
Department of Mechanical Engineering
University of Idaho
Moscow, Idaho, 83843, USA
and
Kutateladze Institute of Thermophysics SB RAS
Novosibirsk, 630090, Russia
Email: aleksei_sakhnov@mail.ru

ABSTRACT

We study the evolution of the solid-liquid interface during melting and solidification of a material with constant internal heat generation and prescribed heat flux at the boundary for a plane wall and a cylinder. The equations are solved by splitting them into transient and steady-state components and then using separation of variables. This results in an ordinary differential equation for the interface that involves infinite series. The initial value problem is solved numerically, and solutions are compared to the previously published quasi-static solutions. We show that when the internal heat generation and the heat flux at the boundary are close in value to each other, the motion of the phase change front takes longer to reach steady-state than when the values are farther apart. As the difference between the internal heat generation and the heat flux increases, the transient solutions become more dominant and the numerical solution of the phase change front does not reach steady-state before the outer boundary or centerline is reached. The difference between the internal heat generation and the heat flux at the boundary can be used to control the motion and speed of the interface.The problem has applications for a nuclear fuel rod during meltdown.

NOMENCLATURE

A_n, B_n Fourier coefficients or Fourier-Bessel coefficients
c_p specific heat
Δh_f latent heat of fusion
k thermal conductivity
L distance from the center to the edge of the plane wall
r_o distance from the center to the edge of the cylinder
$\dot{q}$ volumetric internal heat generation
$\dot{Q}$ dimensionless internal heat generation
$s(t)$ distance to the phase change front
t time
T temperature
q_o'' constant surface heat flux
Q'' dimensionless surface heat flux
T_m melting temperature

x, r distance
J_n Bessel function of the first kind
Y_n Bessel function of the second kind
Z_0 zeros of the Bessel function

Greek Symbols

α thermal diffusivity
η nondimensional distance
ϕ initial temperature profile
Φ nondimensional initial temperature profile
λ_n, $\tilde{\lambda}_n$ characteristic eigenvalues in liquid and solid phases
θ nondimensional temperature
ρ density
τ nondimensional time
$\zeta(\tau)$ nondimensional distance to phase change front

Subscripts

liq liquid
sol solid
ss steady state
tr transient

INTRODUCTION

The classical solid-liquid phase change problem has been studied for over one hundred years, first by Lamé and Clapeyron [1], then by Stefan [2] whose name is now synonymous with this class of problems [3]. While the classical problem has been analyzed, a subset of the problem, namely phase change driven by internal heat generation has been much less studied, even though there are many applications including nuclear energy, thermal energy storage, heat exchangers using phase change materials, geophysics and materials processing.

Various techniques have been used to study phase change driven by internal heat generation including approximate methods [4], perturbation analysis [5], lumped parameter techniques [6], and finite difference methods [7]. One of the primary drivers for this field of study has been nuclear safety analysis. Chen et al. [8] used a simple transient conduction model to determine when a nuclear fuel pin began to melt. El-Genk and Cronenberg [9] studied the effects of internal heat generation on transient freezing in a reactor shield plug using a successive approximation technique. Cheung et al. [10] studied melting and freezing in a heat generating slab between two semi-infinite walls. Chan et al. [11] modeled phase change in semi-transparent materials induced by radiation heat transfer. Chan and Hsu [12] applied the enthalpy method to study the formation of the mushy zone in problems with internal heat generation. Le Tellier, et al. [13] used three different techniques to study the Stefan problem and included the effects of convection in the liquid phase to study the boundary heat flux closure relations. Tang, et al. [14] numerically studied melting processes in a nuclear fuel rod using the half-boundary method applied to an enthalpy formulation. In addition to the melting problem, Dubey and Sharma [15] also modelled the multi-phase flow of nuclear fuel in a fast reactor fuel rod. In this paper, our goal is to present analytical solutions to the Stefan problem with internal heat generation with constant heat flux conditions at the outer wall boundaries.

A discussion is needed about the effect of convection on the propagation of the interface between liquid and solid phases. As research on steel [16–18] shows, the liquid phase adjacent to the solidification front may develop thermally driven flow with estimated velocities of 0.1-1 cm/s [16, 17], while shrinkage due to solidification may give rise to velocity of about 0.01 cm/s [18]. Moreover, the thermal conductivity in the liquid phase with moving liquid could be higher than in a a stagnant liquid. At the same time, the difference is not expected to be large since the heat flow by conduction is much bigger than the heat flow by convection in liquids with low fluid velocities [19]. The Rayleigh number for fluids with low velocities will be small, and therefore, the Nusselt number as the ratio of convective to conductive heat transfer across the boundary will also be small [20, 21]. Moreover, our main application in mind is the meltdown in nuclear fuel rods. Since it takes time to develop convective effects as material melts while melting is fast and remembering that fuel rods are relatively small in size (in radius) and the interface reaches either the outer boundary or the centerline before any significant effect of convection is present, we could assume that convection will not be significant and can be neglected. Experiments to validate this assumption, of course, are needed.

In previous works [22, 23], the behavior of the interface between the liquid and solid phases have been explored in both the plane wall, and cylindrical geometries when the outer-wall temperature is being held constant. In this work, we also consider both geometries but instead of the constant temperature on the outer-wall boundary, we prescribe a constant heat flux. We derived governing equations for the interface between two phases without making a quasi-static assumption and solve the resulting initial value problem numerically. Results from numerical simulations of the full problem are compared to those of quasi-static. Evolution of the interface and temperature in both phases are obtained in solidification and melting regimes.

PROBLEM DESCRIPTION: PLANE WALL

Here, the symmetric plane-wall geometry of the liquid-solid phase change problem with internal heat generation is considered (Fig. 1). In both phases the phase change is driven by the heat generation, $\dot{q}$, and occurs at the same temperature denoted by T_m. In this case, the heat flux at the wall will be held at the constant value q''_o. The temperature gradient at the centerline is zero by symmetry.

In the following solution, the following assumptions were

made:

1. The internal heat generation is constant and the same in both phases
2. The material properties in both phases are constant, uniform, and equal
3. Heat is transferred solely by conduction and there is no convection in the liquid phase
4. The phase change occurs at a single, constant temperature, T_m, so there is no "mushy zone" at the interface in between phases.

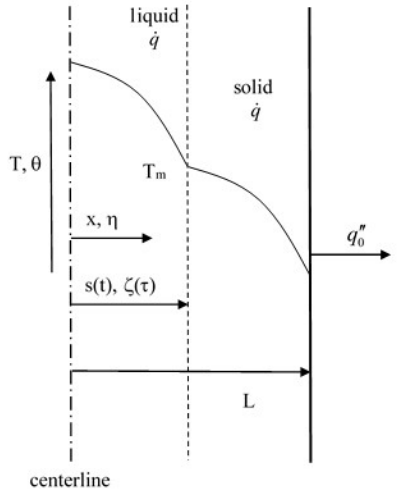

FIGURE 1. SCHEMATIC OF THE PLANE WALL

In both the solid and liquid phases, the behavior is governed by the heat conduction equation:

$$\frac{\partial^2 T(x,t)}{\partial x^2} + \frac{\dot{q}}{k} = \frac{1}{\alpha}\frac{\partial T(x,t)}{\partial t}, \quad 0 \le x \le L, \quad 0 \le t < \infty \tag{1}$$

The boundary and the initial conditions for the liquid phase are

$$\frac{\partial T_{liq}(0,t)}{\partial x} = 0, \quad T_{liq}(s(t),t) = T_m, \quad T_{liq}(x,0) = \phi_{liq}(x)$$

and in the solid phase, the boundary and initial conditions are

$$T_{sol}(s(t),t) = T_m, \quad \left.\frac{\partial T(x,t)}{\partial x}\right|_{x=L} = -\frac{q_o''}{k_{sol}}$$

$$T_{sol}(x,0) = \phi_{sol}(x)$$

Along the interface between two phases, the heat energy balance [24] gives

$$k_{liq}\left.\frac{\partial T_{liq}(x,t)}{\partial x}\right|_{x=s} + \rho_{sol}\Delta h_f \frac{ds(t)}{dt} = k_{sol}\left.\frac{\partial T_{sol}(x,t)}{\partial x}\right|_{x=s} \tag{2}$$

The problem is nondimensionalized by introducing the following dimensionless variables.

$$\eta = \frac{x}{L}, \quad \zeta = \frac{s(t)}{L}, \quad \tau = \frac{\alpha t}{L^2}, \quad \theta(\eta,\tau) = \frac{T(x,t) - T_m}{T^*}$$

$$\dot{Q} = \frac{\dot{q}L^2}{\alpha\rho_{sol}\Delta h_f}, \quad Q'' = \frac{q_o'' L}{\alpha\rho_{sol}\Delta h_f}$$

$$\Phi_{liq}(\eta) = \frac{\phi_{liq}(L\eta) - T_m}{T^*}, \quad \Phi_{sol}(\eta) = \frac{\phi_{sol}(L\eta) - T_m}{T^*}$$

where $T^* = \frac{\alpha\rho_{sol}\Delta h_f}{k_{sol}}$ is a typical temperature obtained by balancing the second and third terms in the interface equation (2).

Using dimensionless variables, the governing equations, boundary and initial conditions are:

$$\frac{\partial^2\theta(\eta,\tau)}{\partial\eta^2} + \dot{Q} = \frac{\partial\theta(\eta,\tau)}{\partial\tau} \tag{3}$$

$$\frac{\partial\theta_{liq}(0,\tau)}{\partial\eta} = 0, \quad \theta_{liq}(\zeta(\tau),\tau) = 0, \quad \theta_{liq}(\eta,0) = \Phi_{liq}(\eta)$$

$$\theta_{sol}(\zeta(\tau),\tau) = 0, \quad \left.\frac{\partial\theta_{sol}(\eta,\tau)}{\partial\eta}\right|_{\eta=1} = -Q''$$

$$\theta_{sol}(\eta,0) = \Phi_{sol}(\eta)$$

$$\left.\frac{\partial\theta_{liq}(\eta,\tau)}{\partial\eta}\right|_{\eta=\zeta} + \frac{d\zeta(\tau)}{d\tau} = \left.\frac{\partial\theta_{sol}(\eta,\tau)}{\partial\eta}\right|_{\eta=\zeta} \tag{4}$$

In order to determine the behavior of the interface, both of the temperature profiles must be found. First we find the solution for the liquid phase. This is done by separating a solution $\theta_{liq}(\eta,\tau)$ into a transient $\theta_{liq,tr}(\eta,\tau)$ and steady-state $\theta_{liq,ss}(\eta)$ parts:

$$\theta_{liq}(\eta,\tau) = \theta_{liq,tr}(\eta,\tau) + \theta_{liq,ss}(\eta) \tag{5}$$

Here the transient solution $\theta_{liq,tr}$ satisfies the corresponding homogeneous problem. This solution is found using separation of variables, whereas the steady-state solution is found by direct integration. The transient solution $\theta_{liq,tr}$ satisfies the following homogeneous heat equation:

$$\frac{\partial^2 \theta_{liq,tr}(\eta,\tau)}{\partial \eta^2} = \frac{\partial \theta_{liq,tr}(\eta,\tau)}{\partial \tau}$$

with homogeneous boundary conditions

$$\frac{\partial \theta_{liq,tr}(0,\tau)}{\partial \eta} = 0, \quad \theta_{liq,tr}(\zeta(\tau),\tau) = 0$$

and the initial condition

$$\theta_{liq,tr}(\eta,0) = \Phi_{liq}(\eta) - \theta_{liq,ss}(\eta)$$

The method of separation of variables produces an infinite series solution

$$\theta_{liq,tr}(\eta,\tau) = \sum_{n=1}^{\infty} A_n \cos(\lambda_n \eta)\, e^{-\lambda_n^2 \tau}$$

with eigenvalues

$$\lambda_n = \frac{-\frac{\pi}{2} + \pi n}{\zeta}, \quad n = 1,2,3,\ldots$$

and associated eigenfunctions $f_n(\eta) = \cos(\lambda_n \eta)$. Fourier coefficients A_n are found by using orthogonality of eigenfunctions $f_n(\eta)$ on $[0,\zeta(\eta)]$:

$$A_n = \frac{2}{\zeta(\tau)} \int_0^{\zeta(\tau)} \left[\Phi_{liq}(\eta) - \theta_{liq,ss}(\eta)\right] \cos(\lambda_n \eta) d\eta$$

The steady-state solution $\theta_{liq,ss}(\eta)$ satisfies

$$\frac{d^2 \theta_{liq,ss}(\eta)}{d\eta^2} = -\dot{Q} \tag{6}$$

and homogeneous boundary conditions

$$\frac{d\theta_{liq,ss}(0)}{d\eta} = 0, \quad \theta_{liq,ss}(\zeta(\tau)) = 0 \tag{7}$$

Integrating equation (6) twice and using boundary conditions (7), we obtain the solution to the steady state part of the problem:

$$\theta_{liq,ss}(\eta) = \frac{\zeta^2 - \eta^2}{2} \dot{Q}$$

Combining transient $\theta_{liq,tr}$ and steady-state $\theta_{liq,ss}$ solutions, we obtain the complete liquid temperature profile:

$$\theta_{liq}(\eta,\tau) = \sum_{n=1}^{\infty} A_n \cos(\lambda_n \eta)\, e^{-\lambda_n^2 \tau} + \frac{\zeta^2 - \eta^2}{2} \dot{Q} \tag{8}$$

We derive the solid phase profile $\theta_{sol}(\eta,\tau)$, $\zeta \le \eta \le 1$, in a similar way as the liquid by applying separation of variables to the transient portion, and integration to the steady-state. The following is the full solid phase temperature profile $\theta_{sol}(\eta,\tau)$

$$\begin{aligned}\theta_{sol}(\eta,\tau) = &\sum_{n=1}^{\infty} B_n \left[\cos(\tilde{\lambda}_n \eta) + \tan(\tilde{\lambda}_n)\sin(\tilde{\lambda}_n \eta)\right] e^{-\tilde{\lambda}_n^2 \tau} \\ &+ \frac{\zeta^2 - \eta^2}{2} \dot{Q} + \left(\dot{Q} - Q''\right)(\eta - \zeta)\end{aligned} \tag{9}$$

where eigenvalues $\tilde{\lambda}_n$ and associated eigenfunctions $\tilde{f}_n(\eta)$ are

$$\tilde{\lambda}_n = \frac{-\frac{\pi}{2} + \pi n}{1 - \zeta}, \quad n = 1,2,3,\ldots$$

$$\tilde{f}_n(\eta) = \cos(\tilde{\lambda}_n \eta) + \tan(\tilde{\lambda}_n)\sin(\tilde{\lambda}_n \eta)$$

Fourier coefficients B_n are found by orthogonality of eigenfunctions $\tilde{f}_n$ on $\eta \in [\zeta, 1]$:

$$B_n = \frac{\int_{\zeta(\tau)}^{1} \left[\Phi_{sol}(\eta) - \theta_{sol,ss}(\eta)\right] \tilde{f}_n(\eta) d\eta}{\int_{\zeta(\tau)}^{1} [\tilde{f}_n(\eta)]^2 d\eta}$$

To find the evolution equation for the interface $\zeta(\tau)$ between two phases, we differentiate temperatures $\theta_{liq}(\eta,\tau)$ and

$\theta_{sol}(\eta,\tau)$ with respect to η, evaluate them at $\eta=\zeta(\tau)$ and substitute into the interface equation (4) to obtain an ordinary differential equation for $\zeta(\tau)$:

$$\frac{d\zeta}{d\tau}=\sum_{n=1}^{\infty}A_n\lambda_n\,\mathrm{e}^{-\lambda_n^2\tau}\sin\lambda_n\zeta+\sum_{n=1}^{\infty}B_n\tilde{\lambda}_n\,\mathrm{e}^{-\tilde{\lambda}_n^2\tau}\,\bar{f}_n(\zeta)+(\dot{Q}-Q'') \tag{10}$$

where $\bar{f}_n(\zeta)=-\sin(\tilde{\lambda}_n\eta)+\tan(\tilde{\lambda}_n)\cos(\tilde{\lambda}_n\eta)$.

QUASI-STATIC SOLUTION: PLANE WALL

When solutions in each phase are time-independent, transient parts of temperature profiles are zero, and the quasi-static solutions are just steady-state solutions. The interface equation (10) simplifies to

$$\frac{d\zeta}{d\tau}=\dot{Q}-Q'' \tag{11}$$

whose solution is readily obtained by integration and using initial condition $\zeta(0)=\zeta_0$:

$$\zeta(\tau)=\left(\dot{Q}-Q''\right)\tau+\zeta_0 \tag{12}$$

which agrees with quasi-static solution obtained in [22]. From here we can see that if $\dot{Q}=Q''$, i.e. the internal heat generation is in balance with the heat flux at the outer boundary, so the interface should not move. If $\dot{Q}>Q''$, we have the internal heat generation stronger than the heat flux at the boundary, and the interface is expected to move to the right until it reaches the boundary at $\eta=1$. For $\dot{Q}<Q''$, the internal heat generation will be weaker than the prescribed heat flux, and the interface would be moving to the left until it reaches the centerline. The bigger difference between $\dot{Q}$ and Q'' is, faster the interface moves.

We expect a similar overall behavior of the interface for the full problem but transient solutions will be dominant at early times. As time increases, the transient solution would approach zero, however, if the interface reaches either the outer boundary or the centerline quickly, the transient solution may not have enough time to decay. As a result, the full problem solution will not approach the quasi-static solution.

PROBLEM DESCRIPTION: CYLINDER

In the cylindrical version of the problem (schematic as seen in Fig. 2) the same four assumptions are made as in the plane wall version. As with the plane wall, the system is naturally symmetrical, the phase change is driven by the internal heat generation $\dot{q}$ and occurs at the melting temperature T_m. As before, the heat flux at the boundary is held constant at q_o''.

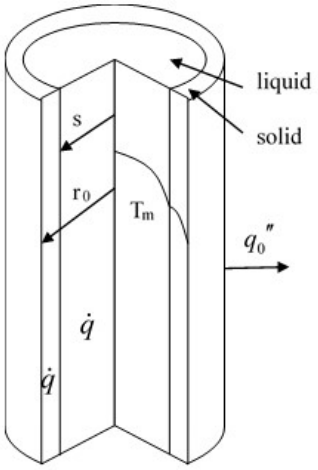

FIGURE 2. SCHEMATIC OF THE PROBLEM IN A CYLINDER

Because of the geometry, it is convenient to use cylindrical coordinates. The heat (1) and the interface (2) equations are

$$\frac{1}{r}\frac{\partial}{\partial r}\left(r\frac{\partial T(r,t)}{\partial r}\right)+\frac{\dot{q}}{k}=\frac{1}{\alpha}\frac{\partial T}{\partial t},\quad 0\le r\le r_0,\quad 0\le t<\infty$$

$$k_{liq}\frac{\partial T_{liq}(r,t)}{\partial r}\Big|_{r=s(t)}+\rho_{sol}\Delta h_f\frac{ds(t)}{dt}=k_{sol}\frac{\partial T_{sol}(r,t)}{\partial r}\Big|_{r=s(t)}$$

The boundary conditions are the same as those imposed on the plane wall geometry: symmetry condition at the centerline of the cylinder, continuity of the temperature at the interface and the prescribed derivative of the temperature at the outer wall. Using the same nondimensionalization as in the plane wall case but with L replaced by r_0, we obtain the following dimensionless heat and interface equations

$$\frac{1}{\eta}\frac{\partial}{\partial\eta}\left(\eta\frac{\partial\theta(\eta,\tau)}{\partial\eta}\right)+\dot{Q}=\frac{\partial\theta(\eta,\tau)}{\partial\tau}$$

$$\frac{\partial\theta_{liq}(\eta,\tau)}{\partial\eta}\Big|_{\eta=\zeta(\tau)}+\frac{d\zeta(\tau)}{d\tau}=\frac{\partial\theta_{sol}(\eta,\tau)}{\partial\eta}\Big|_{\eta=\zeta(\tau)}$$

with the corresponding boundary and initial conditions. Using the same approach for solving a nonhomogeneous problem by

splitting a solution into a transient and steady-state parts (see also [23]), then using the method of separation of variables to find the transient solution and direct integration for the steady-state component, we find

$$\theta_{liq}(\eta,\tau) = \sum_{n=1}^{\infty} A_n \, \mathrm{e}^{-\lambda_n^2 \tau} J_0(\lambda_n \eta) + \theta_{liq,ss}(\eta), \quad 0 \le \eta \le \zeta \tag{13}$$

where

$$\theta_{liq,ss}(\eta) = \frac{\dot{Q}}{4}(\zeta^2(\tau) - \eta^2)$$

$$A_n = \frac{\int_0^{\zeta(\tau)} \left[\Phi_{liq}(\eta) - \theta_{liq,ss}(\eta)\right] J_0(\lambda_n \eta)\eta d\eta}{\int_0^{\zeta(\tau)} {J_0}^2(\lambda_n \eta)\eta d\eta}$$

Here $\lambda_n = \frac{z_{0n}}{\zeta(\tau)}$ are eigenvalues with associated eigenfunctions $f_n(\eta) = J_0(\lambda_n \eta)$, $J_0(z)$ is the Bessel function of the 1st kind of order 0, z_{0n} are zeros of $J_0(z)$, $n = 1,2,3,\ldots$.

We apply the same approach to find solution in the solid phase for $\zeta \le \eta \le 1$. Now, since η is away from zero, solution will also have $Y_0(z)$, the Bessel function of 2nd kind of order 0. We find

$$\theta_{sol}(\eta,\tau) = \sum_{n=1}^{\infty} B_n \, \mathrm{e}^{-\tilde{\lambda}_n^2 \tau} \tilde{f}_n(\eta) + \theta_{sol,ss}(\eta), \quad \zeta \le \eta \le 1 \tag{14}$$

where

$$\theta_{sol,ss}(\eta) = \frac{\dot{Q}}{4}\left(\zeta^2(\tau) - \eta^2\right) + \left(\frac{\dot{Q}}{2} - Q''\right) \ln \frac{\eta}{\zeta(\tau)}$$

the eigenvalues $\tilde{\lambda}_n$, $n = 1,2,3,\ldots$, are roots of the equation

$$J_0(\lambda\zeta)Y_1(\lambda) - Y_0(\lambda\zeta)J_1(\lambda) = 0$$

with associated eigenfunctions

$$\tilde{f}_n(\eta) = J_0(\tilde{\lambda}_n \eta) - \frac{J_1(\tilde{\lambda}_n)}{Y_1(\tilde{\lambda}_n)} Y_0(\tilde{\lambda}_n \eta)$$

and Fourier-Bessel coefficients are

$$B_n = \frac{\int_{\zeta(\tau)}^1 \left[\Phi_{sol}(\eta) - \theta_{sol,ss}(\eta)\right] \tilde{f}_n(\eta)\eta \, d\eta}{\int_{\zeta(\tau)}^1 \tilde{f}_n^2(\eta)\eta \, d\eta}$$

$J_1(z)$, $Y_1(z)$ are Bessel functions of the 1st and 2nd kind of order 1.

Differentiating $\theta_{liq}(\eta,\tau)$ and $\theta_{sol}(\eta,\tau)$ with respect to η, evaluating them at $\eta = \zeta(\tau)$ and using the fact that

$$J_0'(z) = -J_1(z), \quad Y_0'(z) = -Y_1(z)$$

we obtain the following interface equation for $\zeta(\tau)$.

$$\frac{d\zeta}{d\tau} = \sum_{n=1}^{\infty} A_n \lambda_n \, \mathrm{e}^{-\lambda_n^2 \tau} J_1(\lambda_n \zeta) + \sum_{n=1}^{\infty} B_n \tilde{\lambda}_n \, \mathrm{e}^{-\tilde{\lambda}_n^2 \tau} \bar{f}_n(\zeta) + \left(\frac{\dot{Q}}{2} - Q''\right) \frac{1}{\zeta} \tag{15}$$

where

$$\bar{f}_n(\eta) = -J_1(\tilde{\lambda}_n \eta) + \frac{J_1(\tilde{\lambda}_n)}{Y_1(\tilde{\lambda}_n)} Y_1(\tilde{\lambda}_n \eta)$$

Equation (15) is an ordinary differential equation for $\zeta = \zeta(\tau)$ and can be solved numerically to compute the interface. Then equations (13) and (14) can be used to find temperature in both phases.

QUASI-STATIC SOLUTION: CYLINDER

The quasi-static solution for the cylinder can be obtained from equation (15) by letting $\tau \to \infty$ to recover steady-state solutions. This produces

$$\frac{d\zeta}{d\tau} = \left(\frac{\dot{Q}}{2} - Q''\right) \frac{1}{\zeta}$$

Integrating this equation and using the initial condition $\zeta(0) = \zeta_0$, we find

$$\zeta(\tau) = \sqrt{(\dot{Q} - 2Q'')\tau + \zeta_0^2} \tag{16}$$

The result in (16) suggests that in the case of cylinder, the interface ζ behaves like $\tau^{1/2}$, whereas ζ is a linear function of τ in the plane wall case as seen from equation (12). This is in agreement with results in [22].

NUMERICAL SOLUTIONS OF INITIAL BOUNDARY VALUE PROBLEM

We first present numerical solutions of the plane wall case. To analyze the behavior of the interface $\zeta(\tau)$, we solve equation (10) numerically using Matlab software with the ODE solver

`ode23s`. The Fourier series are truncated to 10-20 terms since the eigenvalues are positive and increase, so exponential terms with time decay quickly as time increases and index of an eigenvalue increases. We show the evolution of the interface $\zeta(\tau)$ and temperature profiles in the case when difference between the internal heat generation $\dot{Q}$ and the heat flux value Q'' is small and large. We consider both cases: solidification and melting.

We fix the internal heat generation at $\dot{Q} = 5$. First we study the solidification process when we start from all solid material. To have a physically reasonable solution, the prescribed heat flux Q'' should be larger than $\dot{Q}$. We choose several values of the heat flux Q'' close to $\dot{Q}$, e.g. $Q'' = 5.1$, 5.3 and 5.5. The evolution of the interface ζ as a function of time τ is shown in Fig. 3. For comparison, we plot solutions of the full problem given by the interface equation (10) and plotted using the dashed black line and the quasi-static counterpart (12) plotted with the red solid line. The interface in the quasi-static case is a straight line as a function of τ with the slope $\dot{Q} - Q''$. We can see that for early times, the full solution for all three cases of Q'' differs from the quasi-static as the transient solution dominates but quickly approaches the same slope as quasi-static. This continues until the interface reaches the centerline and all material becomes liquid. In contrast, when the heat flux Q'' is significantly larger than the internal heat generation $\dot{Q}$ as shown in Fig. 4 where $Q'' = 6.5$ and 15, the full solution differs from the quasi-static during the entire process and the difference increases with time. In this case, because of the strong heat flux, the solidification process is fast and the transient solution is large and does not have enough time to decay before the centerline is reached.

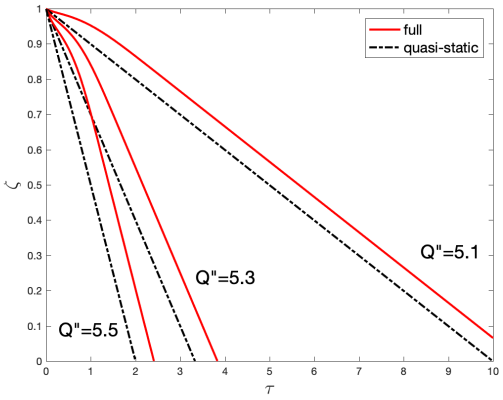

FIGURE 3. INTERFACE EVOLUTION DURING SOLIDIFICATION WITH $Q = 5$ AND $Q'' = 5.1, 5.3$ AND 5.5

In Figs. 5 and 6, we show temperature plots at several different instances of time as time increases again in two cases: with small difference between $\dot{Q}$ and Q'', and large. As can be seen

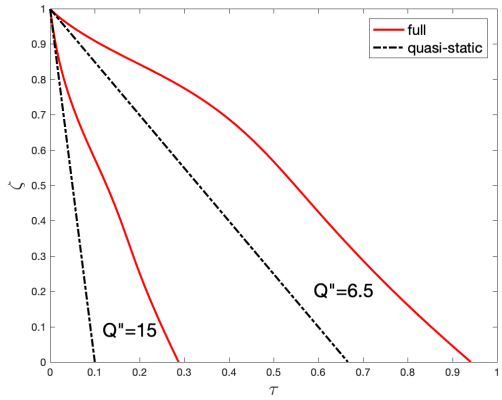

FIGURE 4. INTERFACE EVOLUTION DURING SOLIDIFICATION WITH $Q = 5$ AND $Q'' = 6.5$ AND 15

from Fig. 5, when $\dot{Q}$ and Q'' are close to each other, the temperature in the liquid and solid phases changes smoothly, whereas for the strong heat flux as shown in Fig. 6, the temperature in the solid phase decreases more over time than when the heat flux is close to $\dot{Q}$. As a result, temperature profiles in the liquid and solid phases are continuous but have visibly different slopes at the interface.

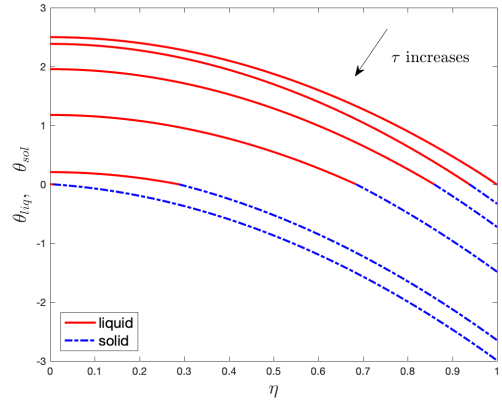

FIGURE 5. TEMPERATURE EVOLUTION IN SOLIDIFICATION CASE WITH $Q = 5$ AND $Q'' = 5.5$ (solid red curve – liquid phase, blue dashed curve – solid phase)

To consider the melting process, we set $\dot{Q} = 5$ again and in this case, the heat flux Q'' should be smaller than $\dot{Q}$. We study two cases here as well: with the heat flux close in value to the internal heat generation and with more significant difference. The evolution of the interface $\zeta(\tau)$ for the case when $Q'' = 4.9$ and 4.5, i.e. Q'' is relatively close to $\dot{Q}$, is depicted in Fig. 7. When $Q'' = 4.9$, the transient solution first brings the full solution away

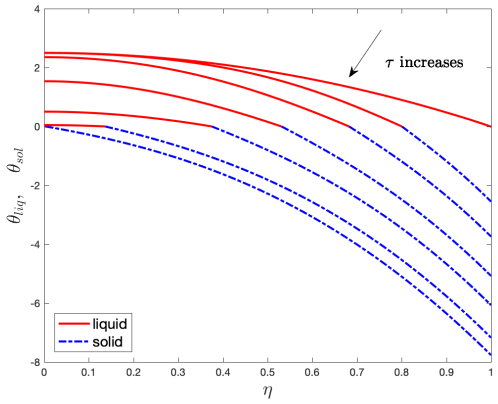

FIGURE 6. TEMPERATURE EVOLUTION IN SOLIDIFICATION CASE WITH $Q = 5$ AND $Q'' = 15$

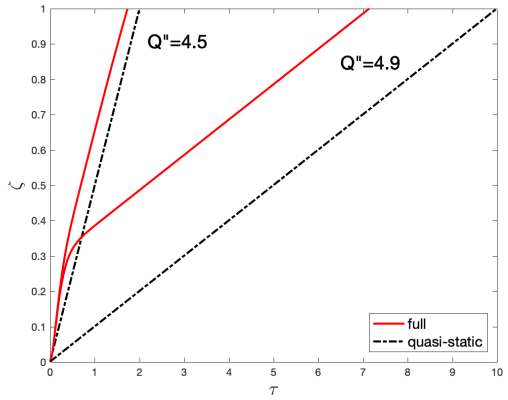

FIGURE 7. INTERFACE EVOLUTION DURING MELTING WITH $Q = 5$ AND $Q'' = 4.9$ AND 4.5

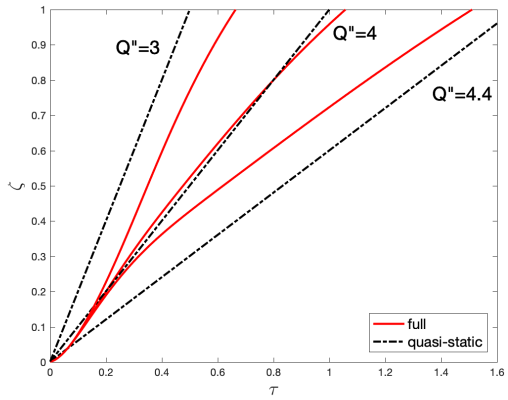

FIGURE 8. INTERFACE EVOLUTION DURING MELTING WITH $Q = 5$ AND $Q'' = 4.4$, 4 AND 3

from the quasi-static but then the full solution follows the same slope as quasi-static. For $Q'' = 4.1$, the heat flux is more different from $\dot{Q} = 5$, so the interface reaches the outer wall faster but overall follows the same slope for later times as quasi-static. The situation is different when the heat flux differs from the internal heat generation more significantly. We consider three cases: $Q'' = 4.3$, 4 and 3, as shown in Fig. 8. In all three cases, transient solutions are quite large during the time of evolution before the interface reaches the outer wall, so the full solution does not exactly follow the quasi-static solution. In addition, as Q'' decreases, i.e. the difference between the $\dot{Q}$ and Q'' increases, the solution to the full problem changes its orientation compared to the quasi-static solution. In particular, when Q'' is close to $\dot{Q}$, the interface from the full problem reaches the outer wall faster than the quasi-static solution. Approximately around $Q'' = 4$, full and quasi-static interfaces move at approximately the same speed. For $Q'' < 4$, the interface from the full problem moves slower than the quasi-static interface. Hence, the value of the heat flux at the outer boundary affects the speed of the interface in the full problem compared to the speed of the quasi-static interface.

In the next two Figs. 9 and 10, we show temperature plots as time increases in two cases: as Q'' is close to $\dot{Q}$ and further away. Fig. 9 shows that when $Q'' = 4.5$, i.e. relatively close to $\dot{Q}$, the temperature in the liquid and solid phases changes smoothly similarly to the solidification case with a small difference between the internal heat generation and the heat flux at the outer boundary.

In Fig. 10, $Q'' = 3$, so the difference $\dot{Q} - Q''$ is larger, as a a result, temperature in the liquid phase increases at a faster rate, as expected. The overall temperature profile is not smooth at the interface as opposed to the small $\dot{Q} - Q''$ difference case shown in 9.

The above results suggest that the value of the heat flux at the outer boundary can be used to control the motion of the interface between liquid and solid phases. It can speed up or slow down the interface evolution.

We also show some solutions for the case of the cylindrical geometry. We fix again $\dot{Q} = 5$. For the solidification, we need $Q'' > \dot{Q}/2$ as can be seen from the form of the quasi-static solution in (16). We choose $Q'' = 2.6$, 3 and 4. Fig. 11 shows the evolution of the interface for these cases. Similarly to the wall case, for Q'' close to $\dot{Q}/2$, the interface quickly approaches the steady-state solution, whereas for Q'' significantly larger than $\dot{Q}/2$, the transient solution dominates and the interface reaches the centerline before it can reach the steady-state.

Fig. 12 presents the evolution of the interface during the melting process for $\dot{Q} = 5$ and $Q'' = 2.4$, 2 and 1.5. For melting, we require $Q'' < \dot{Q}/2$. In all cases shown, the interface reaches the steady-state quickly with $Q'' = 1.5$ having more pronounced transient solution effects since the difference between $\dot{Q}$ and Q''

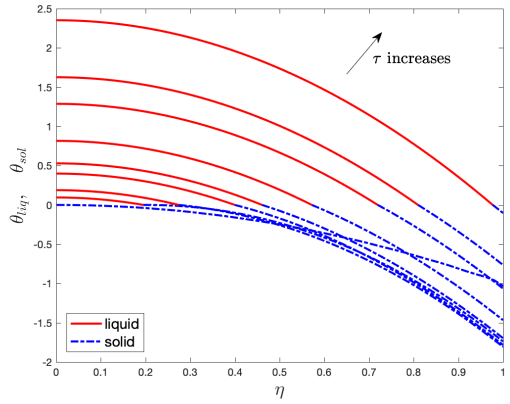

FIGURE 9. TEMPERATURE EVOLUTION IN MELTING CASE WITH $Q = 5$ AND $Q'' = 4.5$

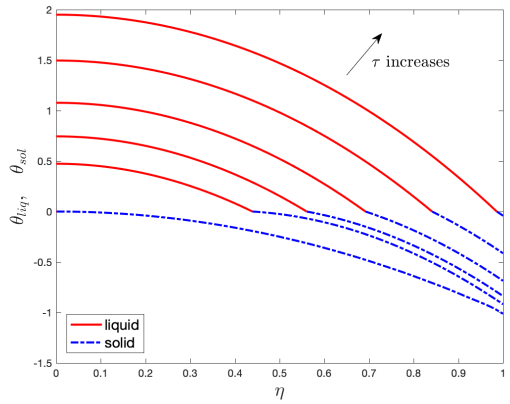

FIGURE 10. TEMPERATURE EVOLUTION IN MELTING CASE WITH $Q = 5$ and $Q'' = 3$

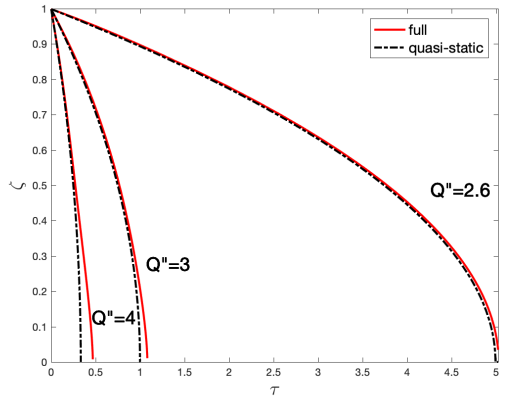

FIGURE 11. INTERFACE EVOLUTION IN A CYLINDER DURING SOLIDIFICATION WITH $Q = 5$ AND $Q'' = 2.6$, 3 AND 4

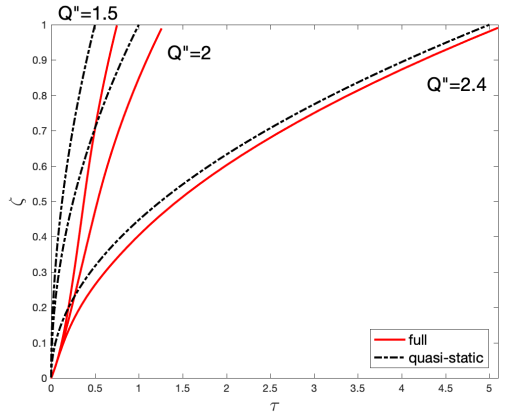

FIGURE 12. INTERFACE EVOLUTION IN A CYLINDER DURING MELTING WITH $Q = 5$ AND $Q'' = 2.4$, 2 AND 1.5

is higher here. When $Q'' = 2.4$, solutions to the full and quasi-static problems are close to each other as expected.

As the profiles for the interface in both solidification and melting processes shown in Figs. 11, 12 suggest, the interface ζ in the full problem behaves like $\tau^{1/2}$ similarly to the quasi-static solution (16).

Conclusions

We consider the problem of solid-liquid phase change with the internal heat generation and prescribed heat flux at the outer boundary in two geometries: a plane wall and a cylinder. Since we have the constant heat flux at the boundary and not the constant temperature, we do not introduce the Stefan number. Instead, we introduce two dimensionless parameters: internal heat generation and the heat flux at the boundary. In both cases, we derive the exact evolution equation for the interface between two phases. The presence of the internal heat generation makes the problem nonhomogeneous, so we solve it by splitting the solution into the transient and steady-state solutions. The transient problem is solved by the method of separation of variables and results in Fourier or Fourier-Bessel series. The steady-state solution is found by the direct integration. The resulting interface equation therefore involves infinite series terms. Since the eigenvalues are positive and increase, time-dependent terms in the infinite series decay quickly and only a few terms can be used to compute solution numerically. We show that when the difference between the internal heat generation and the heat flux at the boundary is small, the temperature changes smoothly. At the same time, the interface quickly approaches a steady-state solution. When this difference is large, temperature gradients at the interface are different, and transient solutions are more dominant at early times causing the interface to reach the outer boundary or the centerline before the steady state can be achieved. We also

show that with the fixed internal heat generation, the heat flux at the outer boundary can be used to control the motion of the interface, in particular its speed.

REFERENCES

[1] Lamé, G., and Clapeyron, B., 1831. "Memoire sur la solidification par refroidissement d'un globe liquide". *Annales Chimie Physique,* ***47***, pp. 250–256.

[2] Stefan, J., 1889. "Ueber die theorie der eisbildung, insbesondere ü ber die eisbildung im polarmeere". *Sitzungsberichte deer k.k. Akademie der Wissenschaften in Wien, Mathematische-Naturwissenschaften, Abteilung II*, pp. 965–983.

[3] Rubenstein, L., 1971. *The Stefan Problem*. AMS Pubs, Providence.

[4] Crepeau, J., and Siahpush, A., 2009. "Approximate solutions to the Stefan problem with internal heat generation". *Heat and Mass Transfer,* ***46***, pp. 787–794.

[5] Yu, Z.-T., Fan, L.-W., Hu, Y.-C., and Cen, K.-F., 2010. "Perturbation solutions to heat conduction in melting or solidification with heat generation". *Heat and Mass Transfer,* ***46***, pp. 479–483.

[6] An, C., and Su, J., 2013. "Lumped parameter model for one-dimensional melting in a slab with volumetric heat generation". *Applied Thermal Engineering,* ***60***, pp. 387–396.

[7] An, C., Moreira, F., and Su, J., 2014. "Thermal analysis of the melting process in a nuclear fuel rod". *Applied Thermal Engineering,* ***68***, pp. 133–143.

[8] Chen, W., Ishii, M., and Grolmes, M., 1976. "Simple heat conduction model with phase change for reactor fuel pin". *Nuclear Science and Engineering,* ***60***, pp. 452–460.

[9] El-Genk, M., and Cronenberg, A., 1978. "An assessment of fuel freezing and drainage phenomena in a reactor shield plug following a core disruptive accident". *Nuclear Engineering and Design,* ***47***, pp. 195–225.

[10] Cheung, F., Chawla, T., and Pedersen, D., 1984. "The effects of heat generation and wall interaction on freezing and melting in a finite slab". *International Journal of Heat and Mass Transfer,* ***27***, pp. 29–37.

[11] Chan, S., Cho, D., and Kocamustafaogullari, G., 1983. "Melting and solidification with internal radiative transfer-A generalized phase change model". *International Journal of Heat and Mass Transfer,* ***26***, pp. 621–633.

[12] Chan, S., and Hsu, K., 1984. *Applications of a generalized phase change model for melting and solidification of materials with internal heat generation*. Proceedings of the AIAA 19th Thermophysics Conference, Snowmass, CO.

[13] Le Tellier, R., Skrzypek, E., and Saas, L., 2017. "On the treatment of plane fusion front in lumped parameter thermal models with convection". *Applied Thermal Engineering,* ***120***, pp. 314–326.

[14] Tang, J., Huang, M., Zhao, Y., Maqsood, S., and Ouyang, X., 2018. "Numerical investigations on the melting process of the nuclear fuel rod in RIAs and LOCAs". *International Journal of Heat and Mass Transfer,* ***124***, pp. 990–1002.

[15] Dubey, A., and Sharma, A., 2018. "Melting and multiphase flow modelling of nuclear fuel in fast reactor fuel rod". *International Journal of Thermal Sciences,* ***125***, pp. 256–272.

[16] Szekely, J., and Stanek, V., 1970. "On heat transfer and liquid mixing in the continuous casting of steel". *Metall. Trans.,* ***1***, pp. 119–126.

[17] Mitsuo, T., Horigome, T., Saito, S., Nomura, E., Kitamuta, Y., and Kono, R., 1981. "On the accumulation mechanism and reducing process of large non-metalic inclusions in the bottom equiaxed zone of ingots". *Tesu-to-Hagane,* ***67***, pp. 1449–1461.

[18] Nomura, H., Tarutani, Y., and Mori, K., 1981. "Mathematical model of formation of segregation zone caused by volume change in solidification of iron steel". *Tetsu-to-Hagane,* ***67***, pp. 1449–1461.

[19] Fujimura, T., Takeshita, K., and Suzuki, R., 2019. "Mathematical analysis of the solidification behavior of multicomponent alloy steel based on the heat- and solute-transfer equations in the liquid-solid zone". *Intern. J. Heat Mass Transfer,* ***130***, pp. 797–812.

[20] Terekhov, V., and Ekaid, A., 2011. "Laminar natural convection between vertical isothermal heated plates with different temperatures". *J. Engr. Thermophys.,* ***20***(4), pp. 416–433.

[21] Terekhov, V., Ekaid, A., and Yassin, K., 2016. "Laminar free convection heat transfer between vertical isothermal plates". *J. Engr. Thermophys.,* ***25***(4), pp. 509–519.

[22] Crepeau, J., and Siahpush, A., 2008. "Approximate solutions to the Stefan problem with internal heat generation". *Heat and Mass Transfer / Waerme- und Stoffuebertragung,* ***44***(7), pp. 787 – 794.

[23] Barannyk, L., Crepeau, J., Paulus, P., and Siahpush, A., 2018. "Fourier-Bessel series model for the Stefan problem with internal heat generation in cylindrical coordinates". In 26th International Conference on Nuclear Engineering ICONE26, July 22-26, London, England, pp. ICONE26–81009.

[24] Poulikakos, D., 1994. *Conduction Heat Transfer*. Prentice-Hall, Englewood Cliffs.